Paper No.
C2020-14667

Influence of the Hardening Phases on the Hydrogen Embrittlement Susceptibility of Ni-Alloys based on UNS N07718

Julia Botinha
VDM Metals International GmbH
Kleffstrasse 23
58762 Altena, Germany

Bodo Gehrmann
VDM Metals International GmbH
Kleffstrasse 23
58762 Altena, Germany

Helena Alves
VDM Metals International GmbH
Kleffstrasse 23
58762 Altena, Germany

ABSTRACT

The Alloy UNS(1) N07718 is among the most used alloys in the oil and gas industry. Due to the presence of the alloying elements niobium, aluminum and titanium, this alloy is precipitation hardenable by the formation of the phases Gamma' and Gamma''. Although presenting excellent strength properties and good resistance in sour gas applications, this material is known to be susceptible to hydrogen embrittlement and most field failures are related to this limiting property.

The use of Alloy 718 (UNS N07718) for oil & gas applications is regulated by the API(2) 6ACRA[1] standard and it is available in three different grades, the 120K, with minimum 120 ksi yield strength, the 140K, with minimum 140 ksi yield strength, and the 150K, with minimum 150 ksi yield strength. Previous studies showed that, due to the different hardening heat treatment parameters, each of the available grades presents a different precipitation behavior in terms of distribution and amount of precipitates, and the obtained microstructure is directly related to the resistance of the material to hydrogen embrittlement.

(1) Unified Numbering System for Metals and Alloys (UNS), SAE International, Warrendale, PA
(2) American Petroleum Institute (API), 1220 L St., N.W., Washington, D.C. 20005-4070

In this context, this study was carried out with the aim of verifying the previous results in heats with modified compositions based on Alloy UNS N07718. The modified compositions were designed to produce microstructures containing different fractions of Gamma' and Gamma''. The presence and fraction of each of the hardening phases were then correlated to the hydrogen embrittlement susceptibility of the material, assessed by means of slow strain rate tests under cathodic application.

Key words: UNS N07718, Alloy 718, Hydrogen Embrittlement, Neutron Diffraction, Hardening Phases, Slow Strain Rate Test

INTRODUCTION

A great number of alloys that can provide good corrosion resistance only achieve high strength properties when cold worked, nevertheless cold worked products are not suitable when thick sections or complex shapes are required. Carbon and low-alloy steels, although having good mechanical properties, do not present enough corrosion resistance. When the application requires thick sections or complex structures, allied with high corrosion resistance, an alloy must be preferentially heat treated to grant more uniform mechanical properties through the cross-section.[2] In the oil and gas industry, Alloy UNS N07718 is found among the most used alloys since it can be precipitation hardened to different high strength conditions by the formation of the phases Gamma' and Gamma'', which are granted by the presence of the alloying elements niobium, aluminum and titanium.

While presenting good mechanical and corrosion properties, the application of alloy UNS N07718 is reported to be limited by the occurrence of hydrogen embrittlement, to which most field failures have been attributed.[3]

Previous studies showed that the strengthening phases Gamma' and Gamma'' play an important role on the corrosion resistance of the alloy UNS N07718.[4-10] Gosheva et al. have made important contributions to clarify the impact of microstructure on the hydrogen embrittlement susceptibility of N07718.[8] Their studies concluded that the amount of hydrogen stored in the material during cathodic hydrogen charging was predominantly dependent on the strengthening precipitates and their interface with the Gamma matrix, which act as trapping sites, slowing down the diffusion process. Klapper et al. showed that the amount and size of precipitates such as Gamma' and Gamma'', as well as the Delta-phase, rather than the strength or hardness level only, predominantly affected the hydrogen embrittlement (HE) susceptibility and defined the type of embrittlement mechanism.[9] According to his studies, HEDE and HELP-assisted shear localization may occur on oil-patch N07718 depending on the amount and localization of Delta-phase.

Due to the different hardening heat treatment parameters, each of the material designations standardized by the API 6ACRA presents a different distribution and particle size of precipitates and the obtained microstructure can be directly related to the resistance of the material to hydrogen embrittlement.[10] Higher volume fractions of Gamma''-precipitates and / or lower volume fractions of Gamma'-precipitates were reported to have deleterious effects on the hydrogen embrittlement resistance.

Even with the variation of the hardening temperatures, as investigated on previous studies,[4-10] material with significant differences in the volume fractions of Gamma' and Gamma'' precipitates cannot be produced. To reach significant differences in the volume fractions of both hardening phases, adaptations must be made on the chemical compositions. TTT Diagrams available in the literature show that the curves representing the formation of Gamma' and Gamma'' in alloy UNS N07718 overlap.[15] In this context, model alloys with chemical-compositions based on Alloy UNS N07718 were developed, with the aim of producing melts containing as much Gamma' as possible and melts containing as much Gamma'' as possible. The model alloys were then tested on Slow Strain Rate Tests (SSRT) under cathodic polarization in order to assess the hydrogen embrittlement susceptibility, so that it was possible to correlate the effect of each phase separately to the embrittlement phenomena.

EXPERIMENTAL PROCEDURE

Material

Four laboratory heats were melted in a Vacuum-Induction-Melting (VIM) laboratory furnace with nominal chemical composition as shown in **Table 1**, where the intentionally modified elements are underlined and in bold. The API 6ACRA composition limits are shown in this table for reference. The ingots were homogenized and hot rolled to sheets with 15 mm (0.6 inch) thickness, which were then solution annealed and age hardened according to the parameters given in **Table 2**.

Thermodynamic Simulations

The occurring phases expected after submitting the alloys to different hardening temperatures and their fractions were calculated for the different alloy variations using the Materials Property Simulation Package JMatPro(3) Version 10.0 from Thermotech,[13] with set cooling rate of 3 °C/s.

(3) Trade name. Java-based Materials Properties.

Heat treatment

The solution annealing and hardening temperatures were defined firstly by thermodynamic simulations and were then experimentally confirmed. Due to the absence of Aluminum, the Heat C required a higher annealing temperature for solution. After solution annealing the microstructures were checked for recrystallization using optical microscopy and all heats were 100% recrystallized. The hardening temperatures were chosen to be those that experimentally resulted in the greatest hardening, given a single-step heat treatment cycle.

Table 1

Nominal chemical composition of laboratory heats

Element	Heat A	Heat B	Heat C	Heat D	API 6ACRA composition limits
C	0.015	0.014	0.014	0.014	0.045 max
S	0.0032	0.0032	0.003	0.0025	0.010 max
Cr	18.49	18.54	18.53	18.55	17.0 to 21.0
Ni	53.6	54.1	53.69	53.77	50.0 to 55.0
Mn	0.01	0.01	0.01	0.01	0.35 max
Si	0.03	0.02	0.03	0.02	0.35 max
Mo	3.05	2.95	3.05	3.02	2.80 to 3.30
Ti	0.95	0.9	0.94	0.93	0.80 to 1.15
Nb + Ta	4.89	**0.02**	5.2	**3.55**	4.87 to 5.20
Cu	0.01	0.01	0.01	0.01	0.23 max
Fe (R)	18.37	22.86	18.53	19.5	Balance
P	0.003	0.003	0.003	0.003	0.010 max
Al	0.51	0.51	**0.01**	0.54	0.40 to 0.60
Mg	0.001	0.001	0.001	0.001	0.0060 max
Ca	0.001	0.001	0.001	0.001	0.0030 max
Co	0.01	0.01	0.01	0.01	1.00 max
B	0.005	0.004	0.005	0.004	0.0060 max

Microstructure

Samples of each laboratory heat were polished and etched with Kallings 2. Microstructural micrographs of the transversal section were obtained by means of Scanning Electron Microscopy (SEM) in order to

check precipitation. SEM was operated at 10 kV accelerating voltage and the free working distance was around 5 mm.

Table 2

Heat treatment parameters of laboratory heats

Heat	Solution annealing			Age hardening		
	Temp [°C (°F)]	Time [h]	Cooling media	Temp [°C (°F)]	Time [h]	Cooling media
A	1032 (1890)	2	Water	760 (1400)	7	Air
B	1032 (1890)	2	Water	770 (1418)	7	Air
C	1045 (1913)	2	Water	770 (1418)	7	Air
D	1032 (1890)	2	Water	750 (1382)	7	Air

Hydrogen Embrittlement Susceptibility Test

In order to evaluate the hydrogen embrittlement susceptibility of the laboratory heats, slow strain rate tests were carried out in test specimens complying with NACE[(4)] TM0198-2011,[11] with gauge section diameter of 3.81 mm (0.15-in) and gauge section length of 25.4 mm (1-in). For each laboratory heat, one specimen was tested in a control environment, which consisted of distilled water purged with nitrogen, and three specimens were tested in an aggressive environment, which consisted of 0.5 M sulfuric acid solution with applied cathodic current density of 5 $mA \cdot cm^{-2}$. Water was selected as the control environment, due to its inertness and the possible better temperature control in comparison to other media such as glycerol and air. No reaction was expected between the distilled water and the material surface. Both solutions were maintained at the temperature of 40°C (104°F) during the tests and the specimens were submitted to a strain rate of $1x10^{-6}$ s^{-1} (crosshead speed $2.5x10^{-5}$ $mm \cdot s^{-1}$). Reduction-of-area, elongation-to-failure, time-to-failure and tensile-strain were reported, as well as the ratios of these values between aggressive and control environments.

A set threshold of 45% for elongation-to-failure-ratio between inert/aggressive environments is used to qualify Alloy UNS N07718 material as acceptable or not acceptable against hydrogen embrittlement.[12] Results greater than the 45% are considered acceptable and the higher this elongation-to-failure-ratio, the less the susceptibility of a material to hydrogen embrittlement.

[(4)] National Association of Corrosion Engineers (NACE) International, 15835 Park Ten Place, Houston, TX 77084

RESULTS AND DISCUSSION

Thermodynamic Simulations

The occurring phases and their fractions in wt.% after age hardening at the temperature corresponding to the greatest hardening, when the material has the higher mechanical properties, were calculated for the different alloy compositions. The calculated fraction of the hardening phases precipitated in each alloy is summarized on **Table 4.**

Table 4

Numerically calculated fraction of Gamma' and Gamma'' precipitates present for each alloy composition

Heat	A	B	C	D
Fraction of Gamma' [%]	9.26	4	3.87	9.02
Fraction of Gamma'' [%]	8.5	0	11.47	4.34

The numerically calculated fractions of Gamma' and Gamma'' phases in the reference composition (corresponding to the reference laboratory heat A) are comparable to values from previous studies. Botinha et al. demonstrated, by means of neutron diffraction methods, that Alloy UNS N07718, when age hardened at 760 °C (1400 °F), the known temperature for peak mechanical properties, precipitates fractions of Gamma' and Gamma'' both in the order of 13%,[10] and comparable results are reported here.

As expected, the heat B, which does not have niobium additons, should precipitate only Gamma', since the presence of only aluminum and titanium as hardening-phase-formation elements should favor the formation of Gamma' phase. However, annulling the content of niobium and considering that the existing aluminum content on the reference material is already low (in the range of 0.5%), a very low quantity of 4% Gamma' is expected to precipitate.

According to the calculations, heat C precipitates mainly Gamma'' with a much lower fraction of Gamma', since Gamma'' is mainly formed by the combination between niobium and nickel. The small fraction of Gamma'-phase expected to form on heat C is due to the substitution of aluminum atoms by titanium and a small fraction of niobium for the formation of the fcc Gamma'-phase.

In order to produce materials with comparable precipitation scenarios, a fourth variation with reduced niobium content was melted (heat D). With a niobium content reduced to around 3.5%, heat D contains both Gamma' and Gamma'' precipitates, but in quantities opposite to in heat C, which allows a more suitable evaluation of the response of each phase's presence to hydrogen embrittlement.

Microstructure

Representative micrographs of a transversal cut of the sheets showing the present precipitates obtained by SEM are shown in **Figures 1 to 4**. For each laboratory heat, micrograph of the representative bulk phases at 50k and 30k magnification were produced.

The identification of both Gamma' and Gamma'' phases through SEM images is not trivial and therefore the SEM analysis is shown for information only. Gamma' particles are known to precipitate with a point-shape while Gamma'' particles are usually found with a linear shape. An attempt to exemplify the both particle formats was made on Figure 1 by the use of yellow arrows.

High temperature phase expected to be Delta-phase was detected on grain boundaries of heat C, what was attributed to the higher availability of niobium in the matrix.

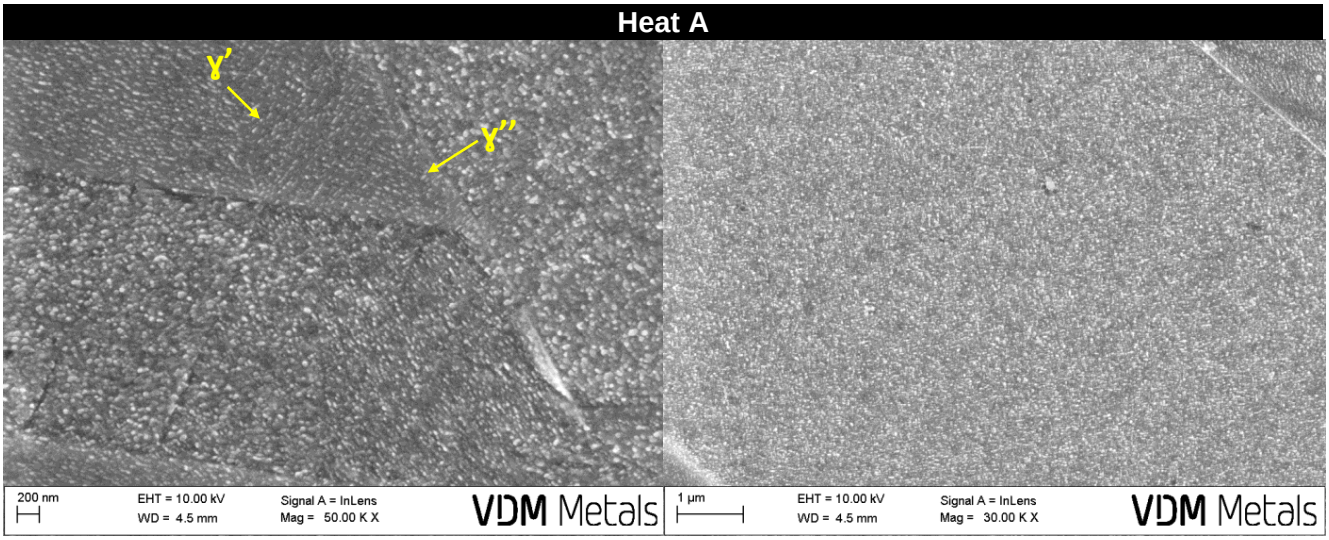

Figure 1: SEM images of laboratory heat A (reference) showing the precipitates after age hardening at 760 °C for 7 hours.

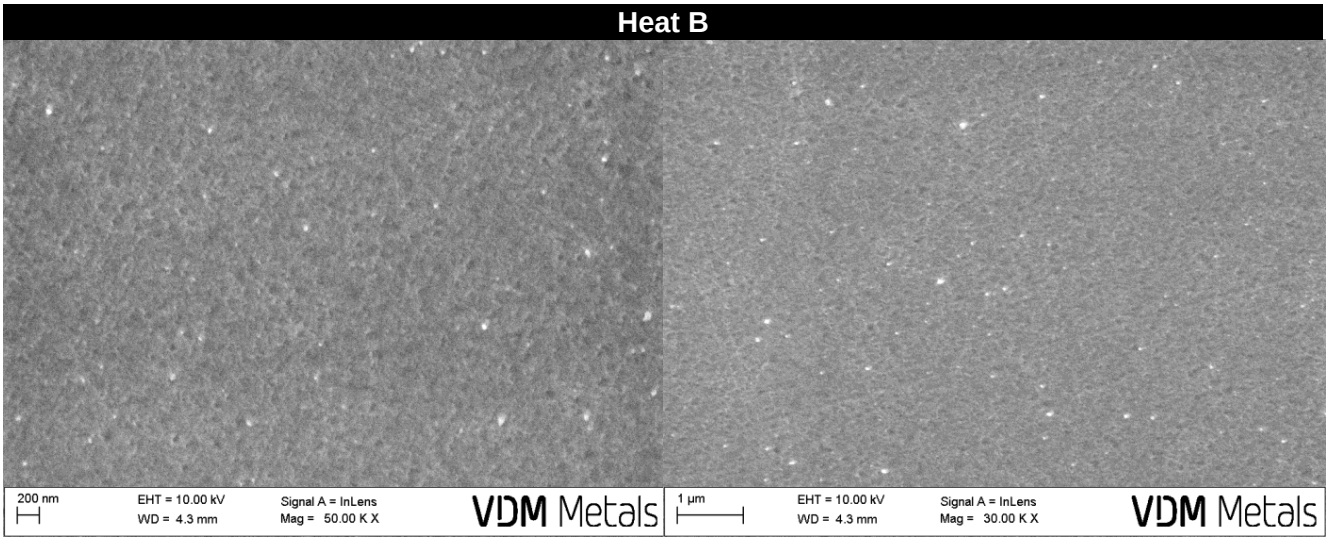

Figure 2: SEM images of laboratory heat B (without Nb) showing the precipitates after age hardening at 770 °C for 7 hours.

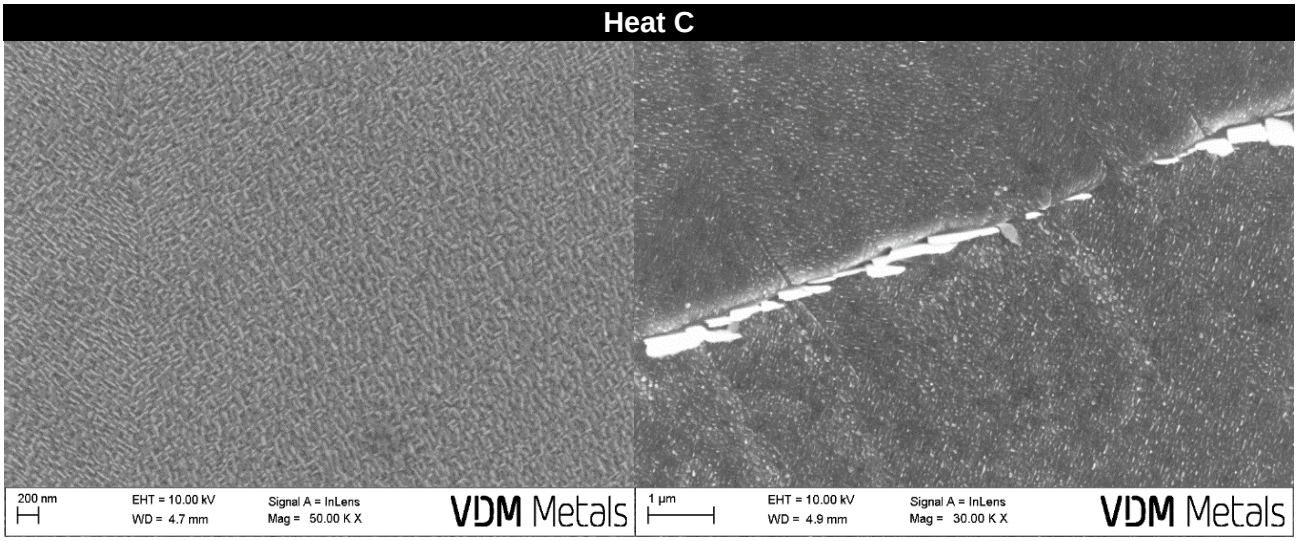

Figure 3: SEM images of laboratory heat C (without Al) showing the precipitates after age hardening at 770 °C for 7 hours.

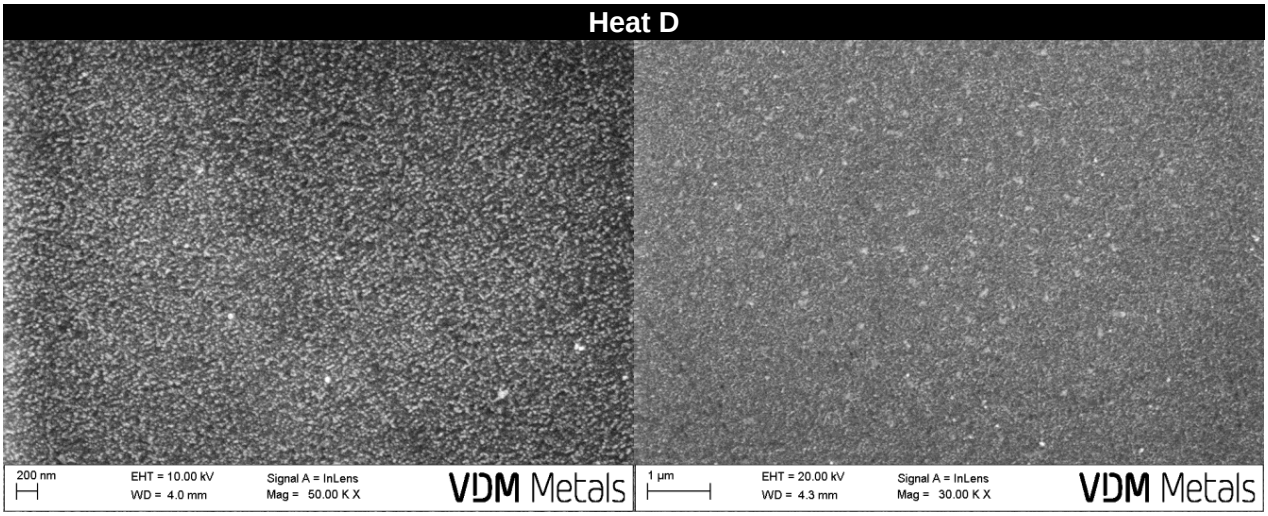

Figure 4: SEM images of laboratory heat D (low Nb) showing the precipitates after age hardening at 750 °C for 7 hours.

Hydrogen Embrittlement Susceptibility Test

The susceptibility of the alloys to hydrogen embrittlement was evaluated by means of SSRT. When comparing the ductility parameters determined for the samples tested in aggressive environment with those of samples tested in control (inert) environment, ductility ratios were calculated and the loss in ductility was used to rate the resistance to the embrittlement caused by the hydrogen. The lower the elongation-to-failure ratio, the higher the sensitivity to hydrogen embrittlement. Detailed SSRT results are presented on **Table 3**, where RoA is the Reduction of Area, ETF is the Elongation to Failure, TTF is the time to failure and Rm is the Tensile Strength. **Figure 5** shows a diagram for comparison of the average elongation-to-failure ratios of the different alloy compositions to the elongation-to-failure ratio of Alloy UNS N07718 in the 140K material designation, which is available in the literature,[10] when standard production material was tested at the same conditions which were used for the present studies. The values regarding the 140K material designation were selected as a reference for this study, since this is the grade that corresponds to the higher mechanical properties achieved by a single-step age hardening and therefore could be directly compared to the laboratory melts, regarding the heat treatment parameters.

Heat A, reference laboratory heat, with chemical analysis in accordance with the API 6ACRA for the UNS N07718, presented an average elongation-to-failure ratio of 64.7%. This value goes well with the expected, given Alloy UNS N07718, aged to the peak of mechanical properties after a single-step ageing (corresponding to the 140K grade of API 6ACRA), presented, in the literature, elongation-to-failure ratios of around 70%.[10, 14]

Table 3

Hydrogen embrittlement susceptibility SSRT test results

Heat	Test Environment	Sample-Nr	RoA		ETF		TTF		Rm	
			[%]	Ratio [%]	[%]	Ratio [%]	min	Ratio [%]	MPa	Ratio [%]
A	inert	A1	26.5	-	20.3	-	4657	-	1109	-
	aggressive	A2	30.1	113.6	13.2	65.0	3295	70.8	1118	100.8
	aggressive	A3	19.6	74.0	13.2	65.0	3448	74.0	1092	98.5
	aggressive	A4	23.4	88.3	13	64.0	3375	72.5	1062	95.8
		Average		**91.9**		**64.7**		**72.4**		**98.3**
B	inert	B1	54.6	-	40.9	-	9098	-	535	-
	aggressive	B2	52.6	96.3	44.9	109.8	9283	102.0	586	109.5
	aggressive	B3	55.7	102.0	44.8	109.5	9442	103.8	487	91.0
	aggressive	B4	62.2	113.9	43	105.1	9039	99.4	513	95.9
		Average		**104.1**		**108.1**		**101.7**		**98.8**
C	inert	C1	46.1	-	17.8	-	4222	-	1108	-
	aggressive	C2	17.2	37.3	9.3	52.2	2524	59.8	1094	98.7
	aggressive	C3	21.7	47.1	10	56.2	2450	58.0	1088	98.2
	aggressive	C4	23.5	51.0	7.8	43.8	2055	48.7	1038	93.7
		Average		**45.1**		**50.7**		**55.5**		**96.9**
D	inert	D1	53.8	-	30.5	-	6343	-	973	-
	aggressive	D2	38.4	71.4	28.4	93.1	5934	93.6	937	96.3
	aggressive	D3	34.9	64.9	26.2	85.9	5838	92.0	882	90.6
	aggressive	D4	42.1	78.3	31	101.6	6213	98.0	895	92.0
		Average		**71.5**		**93.6**		**94.5**		**93.0**

The laboratory heat B (without Niobium addition), did not show any susceptibility to Hydrogen Embrittlement, since the elongation-to-failure ratios are higher than 100%. This value means that the material does not lose ductility after being exposed to the hydrogen charged medium. The low tensile strength values are mostly due to the absence of the hardening phase Gamma'' and the low amount of precipitated particles, which are responsible for hardening and improved tensile properties of the material.

It is not uncommon that ratios higher than 100% are obtained for materials resistant to Hydrogen Embrittlement, considering the existence of a standard deviation for the measurements. Test on inert medium was repeated and no deviation from the values of the first sample was observed.

With a chemical composition free of Aluminum, the laboratory heat C is the most susceptible to hydrogen embrittlement, showing an elongation-to-failure ratio of 50.7% in average. Delta-phase

precipitation was detected on the grain boundaries, what explains the generally reduced ductility of the material, due to the weak interface between precipitate and matrix. However, according to previous studies, an increasing amount of Delta-phase on Alloy UNS N07718 until a certain amount was not deleterious to the Hydrogen Embrittlement behavior of the material.[9,16] Therefore, the low Elongation-to-failure ratio was attributed to the amount of Gamma''-phase in this heat.

Heat D presented an elongation-to-failure-ratio of 93.6%. The small loss in ductility after exposure to the hydrogen charged medium was correlated to the presence of Gamma'' particles in smaller amounts, when compared to the standard compositions of UNS N07718. This combination of low niobium and usual aluminum content assured an improved resistance against Hydrogen Embrittlement while maintaining good mechanical properties and ductility.

Taking in consideration the both reference values for Alloy UNS N07718 – the production heat in the 140K grade from the literature[10] and the reference laboratory heat A – and comparing it with the characteristics of the laboratory heats B, C and D, it can be assumed that the higher the proportion Gamma' / Gamma'', the higher the resistance of the alloys to hydrogen embrittlement.

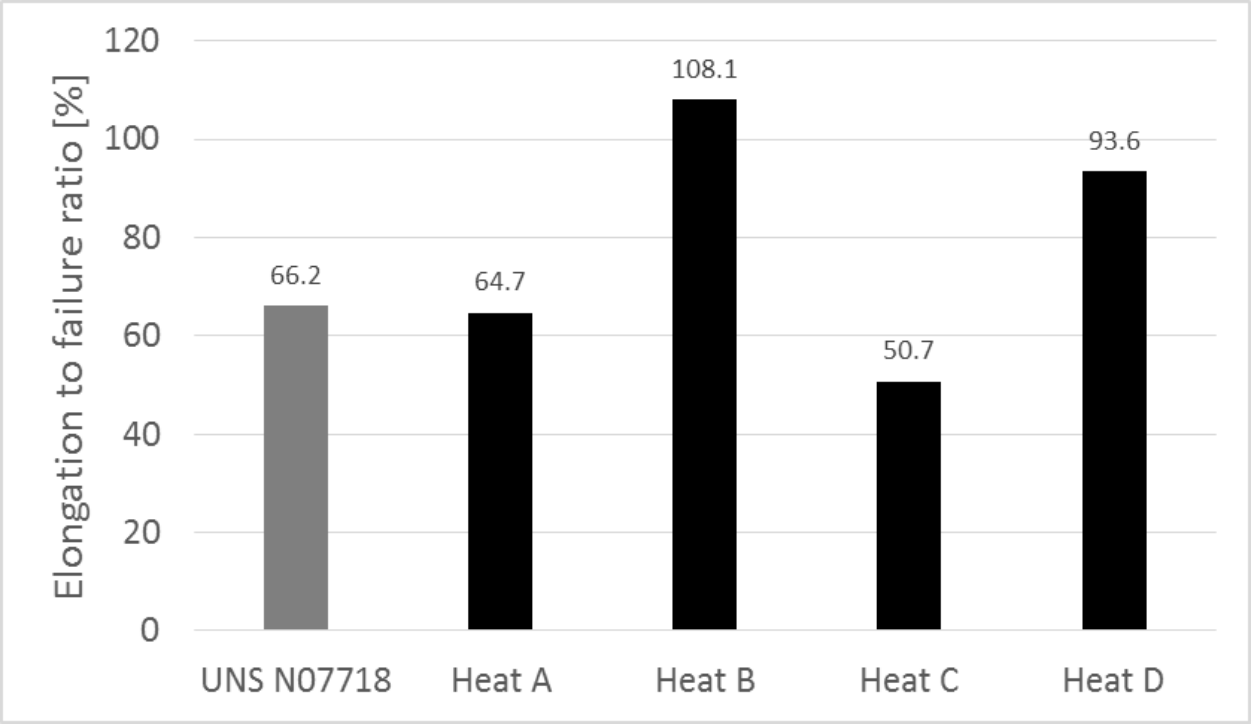

Figure 5: Elongation-to-failure ratio of model alloys in comparison to production heat of Alloy UNS N07718 in the 140K Material Designation available in the literature [10]

CONCLUSIONS

Model alloys with microstructures containing more of one or another hardening phase, i.e. Gamma' and Gamma'', allowed the confirmation of the theory developed on previous works that the hardening phases play an important role on the Hydrogen Embrittlement resistance of Alloy UNS N07718.

It could be concluded that the ordered fcc Gamma'-phase was not responsible for the embrittling behavior of the model alloys, since material presenting only this phase on the microstructure did not present any reduction in ductility after being strained under the aggressive environment. Additionally, materials with a high fraction of Gamma' presented less susceptibility to Hydrogen Embrittlement than materials in the opposite condition, which have a lower fraction of Gamma'.

On the other hand, the results showed that the bcc tetragonal Gamma''-phase may play an important role on the embrittlement of these materials. The ductility of material containing mainly Gamma''-phase on its microstructure (Heat C, although presenting also Delta-phase decoration on grain boundaries) greatly decreases after being strained under aggressive environment, and as the amount of Gamma''-phase was reduced, as on heat D, an increase of elongation-to-failure ratios was seen.

In despite of this negative effect, Gamma'' and therefore the addition of niobium, showed to be essential to grant to the Alloy UNS N07718 the desired high mechanical properties. Only Gamma' in the low amounts achieved by heat B is not able to harden the material properly, as noted on the tensile strength values on slow strain ratio tests.

The presence of intergranular precipitation can be detrimental to the mechanical properties, although these studies did not allow their correlation to the susceptibility to Hydrogen Embrittlement.

Further investigations are running to quantify the volume fraction of the different phases for each laboratory heat through Neutron Diffraction techniques.

AKNOWLEDGEMENTS

The authors would like to thank Fabian Ramlau for the good work to produce SEM micrographs within the labs of VDM Metals. Further thanks to the Salzgitter Mannesmann Research Institute for carrying out all corrosion tests.

REFERENCES

1. API Standard 6ACRA, First Edition (August 2015), "Age-hardened Nickel-based Alloys for Oil and Gas Drilling and Production Equipment" (Washington, NW: API Publishing Services).

2. J. Kolts, “Alloy 718 for the oil and gas industry”. Superalloy 718 – Metallurgy and Applications. The Minerals, Metals & Society, 1989.
3. S.Huizinga, B. McLoughlin, W.E. Like and J.G. de Jong. “Offshore nickel alloy tubing hanger and duplex stainless steel piping failure investigations”, NACE Corrosion 2003, Paper no. 03129 (Houston, USA: NACE, 2003)
4. 5. B. Kagay, K. Findley, S. Coryell, A.B. Nissan, “Effects of alloy 718 microstructure on hydrogen embrittlement susceptibility for oil and gas environments”, Material Science and Technology Vol. 32, No 7-8 (2016): 697-707.
5. 6. L. Liu, K. Tanaka, A. Hirose, K. F. Kobayashi, “Effects of precipitation phases on the hydrogen embrittlement sensitivity of Inconel 718,” Science and Technology of Advanced Materials 3 (2002): 335-344.
6. 7. Z. Guo, M. Zhao, C, Li, S. Chen, L. Rong, Mechanism of hydrogen embrittlement in a gamma-prime phase strengthened Fe-Ni based austenitic alloy”, Elsevier, Materials Science and Engineering A 555 (2012) 77-84
7. 8. M. C. Rezende, L. S. Araujo, S. B. Gabriel, D. S. dos Santos, L. H. de Almeida, “Hydrogen embrittlement in nickel-based superalloy 718: Relationship between γ´+ γ´´ precipitation and the fracture mode,” International Journal of Hydrogen Energy 40 (2015): 17075-17083
8. O. Gosheva, G. Anderson, M. Oechsner, J. Klöwer, A. Aghajani, “Impact of microstructure on hydrogen solubility and diffusivity in UNS 07718”, CORROSION/2016, paper no. 7267 (Houston, TX: NACE 2016)
9. Sarmiento Klapper H, Klöwer J, Gosheva O. 2017 Hydrogen embrittlement: the game changing factor in the applicability of nickel alloys in oilfield technology. Phil. Trans. R. Soc. A 375: 20160415.
10. J. Botinha, B. Gehrmann, H. Alves, R. Gilles, C. Solís, J. Munke, A. Feoktystov, V. Baran. “Study of Phase Distribution on Alloy UNS N07718 in Different Hardening Conditions and Ist Relationship with Hydrogen Embrittlement Susceptibility”. NACE Corrosion 2019, Paper no. 13025 (Houston, USA: NACE, 2019)
11. NACE TM0198-2011, “Slow Strain Rate Test Method for Screening Corrosion-Resistant Alloys (CRAs) for Stress Corrosion Cracking in Sour Oilfield Service”, (Houston, TX: NACE International)
12. L. Foroni, “Hydrogen Embrittlement Susceptibility of Precipitation Hardened Ni-Alloys”, CORROSION/2014, paper no. 3948 (Houston, TX: NACE, 2014).
13. N. Saunders, Z. Guo, X. Li, A. P. Miodownik and J-Ph. Schillé, “Modelling the Material Properties and Behaviour of Ni-Based Supperalloys”. Superalloys 2004, TMS (the Minerals, Metals & Materials Society), 2004.
14. J. Rosenberg, J. Klöwer, J. Groth, C. Bosch, G. Genchev. „Effect of heat treatment on mechanical properties and corrosion resistance of Nickel Alloy UNS N07718 – 140 ksi and 150 ksi grades“. NACE Corrosion 2018, Paper No. 10650 (Houston, USA: NACE, 2018).
15. A. Oradei-Basile and J.F Radavich, “A Current T-T-T Diagram for Wrought Alloy 718” Superalloys 718, 625 and Various Derivatives, Edited by Edward A. Loria. The Minerals, Metals & Materials Society, 1991.
16. O. Gosheva, “Effect of the microstructure of nickel alloy UNS N07718 on its corrosion behavior” (doctor thesis, Darmstadt, GE, 2018)